Published OnlineFirst January 26, 2010; DOI: 10.1158/0008-5472.CAN-09-4043

Therapeutics, Targets, and Chemical Biology

Cancer Research

PERK–Dependent Regulation of Ceramide Synthase 6 and Thioredoxin Play a Key Role in *mda*-7/IL-24–Induced Killing of Primary Human Glioblastoma Multiforme Cells

Adly Yacoub[1], Hossein A. Hamed[1], Jeremy Allegood[1], Clint Mitchell[1], Sarah Spiegel[1], Maciej S. Lesniak[7], Besim Ogretmen[8], Rupesh Dash[3], Devanand Sarkar[3,4], William C. Broaddus[5], Steven Grant[1,2,4], David T. Curiel[6], Paul B. Fisher[3,4], and Paul Dent[1,4]

Abstract

Melanoma differentiation associated gene-7(*mda*-7) encodes IL-24, a cytokine that can selectively trigger apoptosis in transformed cells. Recombinant *mda*-7 adenovirus (Ad.*mda*-7) effectively kills glioma cells, offering a novel gene therapy strategy to address deadly brain tumors. In this study, we defined the proximal mechanisms by which Ad-*mda*-7 kills glioma cells. Key factors implicated included activation of the endoplasmic reticulum stress kinase protein kinase R–like endoplasmic reticulum kinase (PERK), Ca^{++} elevation, ceramide generation and reactive oxygen species (ROS) production. PERK inhibition blocked ceramide or dihydroceramide generation, which were critical for Ca^{++} induction and subsequent ROS formation. Activation of autophagy and cell death relied upon ROS formation, the inhibition of which ablated Ad.*mda*-7–killing activity. In contrast, inhibiting TRX induced by Ad.MDA-7 enhanced tumor cytotoxicity and improved animal survival in an orthotopic tumor model. Our findings indicate that *mda*-7/IL-24 induces an endoplasmic reticulum stress response that triggers production of ceramide, Ca^{2+}, and ROS, which in turn promote glioma cell autophagy and cell death. *Cancer Res; 70(3); 1120–9. ©2010 AACR.*

Introduction

In the United States, glioblastoma multiforme (GBM) is diagnosed in ~20,000 patients per annum. High-grade tumors such as anaplastic astrocytoma and GBM account for the majority of tumors (1). Even when all of the tumor can be surgically removed and patients are maximally treated with radiation and chemotherapy, the mean survival is only extended from ~3 to ~12 months (1).

The melanoma differentiation–associated gene-7/ interleukin 24 (*mda-7*/IL-24) gene was isolated from human melanoma cells induced to undergo terminal differentiation by IFN and mezerein treatment (2). MDA-7/IL-24 protein expression is decreased in advanced melanomas, with undetectable levels in metastatic disease (2–4). This cytokine is a member of the interleukin-10 (IL-10) family (5–12). Enforced expression of MDA-7/IL-24 by a recombinant adenovirus Ad.*mda-7* inhibits growth and kills a broad spectrum of cancer cells without exerting deleterious effects in normal human epithelial or fibroblast cells (9–14). Considering its potent cancer-specific apoptosis-inducing ability and tumor growth–suppressing properties in xenograft models, *mda-7*/IL-24 was evaluated in a phase I trial (10, 11, 15, 16). This study indicated that Ad.*mda-7* injected intratumorally was safe, and with repeated injection, significant clinical activity was evident.

The apoptotic pathways by which Ad.*mda-7* causes cell death are not fully understood; however, current evidence suggests an inherent complexity and an involvement of proteins important for the onset of growth inhibition and apoptosis, including BCL-XL, BCL-2, and BAX (9–14). In melanoma cell lines, but not in normal melanocytes, Ad.*mda-7* infection induces a decrease in BCL-2 and BCL-XL levels, with a modest upregulation of BAX and BAK expression (17). The ability of Ad.*mda-7* to induce apoptosis in DU-145 prostate cancer cells, which do not produce BAX, indicates that MDA-7/IL-24 could also mediate apoptosis by a BAX-independent pathway (9–12). Overexpression of BCL-2 or BCL-XL protects cells from Ad.*mda-7*–induced toxicity in a cell type–dependent fashion (18). In one ovarian cancer line, MDA-7/IL24 was reported to kill via the extrinsic apoptosis pathway (19). Thus, MDA-7/IL-24 lethality seems to occur by multiple distinct pathways in different cell types, but in all of these studies, killing is reflected in a profound induction of mitochondrial dysfunction (20).

The ability of MDA-7/IL-24 to modulate cell signaling processes in transformed cells has been investigated by several groups (13–32). Our laboratories have shown that Ad.*mda-7* kills melanoma cells, in part, by promoting p38

Authors' Affiliations: Departments of [1]Biochemistry and Molecular Biology, [2]Medicine, [3]Human and Molecular Genetics, [4]VCU Institute of Molecular Medicine, [5]Neurosurgery, Virginia Commonwealth University, School of Medicine, Richmond, Virginia; [6]Division of Human Gene Therapy, University of Alabama, Birmingham, Alabama; [7]Brain Tumor Center, The University of Chicago, Chicago, Illinois; and [8]Medical University of South Carolina, Charleston, South Carolina

Note: Supplementary data for this article are available at Cancer Research Online (http://cancerres.aacrjournals.org/).

Corresponding Author: Paul Dent, Department of Biochemistry and Molecular Biology, Massey Cancer Center, Virginia Commonwealth University, Box 980035, 401 College Street, Richmond, VA 23298-0035. Phone: 804-628-0861; Fax: 804-827-1309; E-mail: pdent@vcu.edu.

doi: 10.1158/0008-5472.CAN-09-4043

Published OnlineFirst January 26, 2010; DOI: 10.1158/0008-5472.CAN-09-4043

mitogen-activated protein kinase (MAPK)–dependent activation of the growth arrest and DNA damage–inducible genes, including GADD153 and GADD34 (27). In primary GBM cells, however, we noted p38 MAPK signaling as a protective signal (25). Other groups have argued that inhibition of phosphoinositide-3-kinase signaling, but not ERK1/2 signaling, modestly promotes Ad.*mda-7* lethality in breast and lung cancer cells (28–30).

MDA-7/IL-24 toxicity has been linked to alterations in endoplasmic reticulum (ER) stress signaling (21). In addition to virus-administered *mda-7*/IL-24, delivery of this cytokine as a bacterially expressed glutathione *S*-transferase fusion protein, GST-MDA-7, retains cancer-specific killing, selective ER localization, and induces similar signal transduction changes in cancer cells. We have noted that high concentrations of GST-MDA-7/IL-24 or infection with Ad.*mda-7* kills human glioma cells in an ER stress–dependent fashion that is contingent on mitochondrial dysfunction (22–25). The present studies have elucidated in detail the proximal mechanisms downstream of Ad.*mda-7*–induced ER stress that mediate MDA-7/IL-24 toxicity.

Materials and Methods

Materials

Antibodies were purchased from Cell Signaling Technologies and Santa Cruz Biotechnology. *N*-acetyl cysteine was supplied by Calbiochem. Media and penicillin-streptomycin were purchased from Life Technologies. Dr. David Guis (Radiation Oncology Branch National Cancer Institute Bethesda, MD) supplied the TR/TRX plasmids. The plasmids to express BiP/GRP78 and calbindin D28 were provided by Dr. A. Lee (Department of Biochemistry and Molecular Biology, Keck School of Medicine, USC/Norris Comprehensive Cancer Center, Los Angeles, CA), and Dr. Y.J. Oh (Yonsei University, Seoul, South Korea), respectively.

Methods

***Generation of Ad.*mda-7.** Recombinant serotype 5 adenoviruses to express MDA-7 (Ad.*mda-7*) and control (Ad.*cmv* vector) were generated using recombination in HEK293 cells (14).

***Cell culture and* in vitro *infection of cells with Ad.*mda-7.** All lines were cultured at 37°C (5% v/v CO_2) *in vitro* using RPMI supplemented with 5% (v/v) FCS. Primary human glioma cells were subcultured in 2% (v/v) FCS for 1 wk prior to *in vitro* analyses, after which cells were cultured in 5% serum. For short-term cell-killing assays and immunoblotting, cells were plated at a density of 3×10^3 per cm^2 and 24 h after plating were infected [Ad.*cmv*; Ad.*mda-7* (GBM6 and GBM14 at 10 multiplicity of infection; GBM12 at 25 multiplicity of infection)] and the expression of the recombinant viral transgene allowed to occur for 24 h prior to any additional procedure, including irradiation (4 Gy). *In vitro* inhibitor treatments were from a 100 mmol/L stock solution of each drug and the maximal concentration of vehicle (DMSO) in medium was 0.02% (v/v).

Cell treatments, SDS-PAGE, and Western blot analysis. For SDS-PAGE and immunoblotting, cells were lysed in either a nondenaturing lysis buffer, and prepared for immunoprecipitation as described (33), or in whole-cell lysis buffer [0.5 mol/L Tris-HCl (pH 6.8), 2% SDS, 10% glycerol, 1% β-mercaptoethanol, and 0.02% bromophenol blue], and the samples were boiled for 30 min. The boiled samples were loaded onto 10% to 14% SDS-PAGE and electrophoresis was run overnight. Proteins were electrophoretically transferred onto 0.22 μm nitrocellulose, and immunoblotted with the indicated primary antibodies against different proteins.

***Recombinant adenoviral vectors; infection* in vitro.** We generated and purchased adenoviruses to express constitutively active MEK1 EE, constitutively active AKT, dominant negative MEK1, dominant negative caspase 9, CRM A, and BCL-XL (Vector Biolabs). Cells were infected with these adenoviruses at a multiplicity of infection of 50. Cells were further incubated for 24 h prior to ensure adequate expression of transduced gene products (23–25).

Detection of cell death by trypan blue, terminal deoxynucleotidyl transferase–mediated dUTP nick end labeling, and flow cytometric assays. Trypan blue, Annexin V/propidium iodide, and terminal deoxynucleotidyl transferase–mediated dUTP nick end labeling assays were carried out in triplicate to determine cell viability (24–26).

Plasmid transfection. Plasmid DNA was transfected using LipofectAMINE 2000 reagent (Invitrogen) according to the instructions of the manufacturer.

Microscopy for LC3-GFP expression. Twelve hours after transfection, LC3-green flourescence protein (GFP)–transfected cells were infected (where indicated) with either Ad.*cmv* or Ad.*mda-7*, and then cultured for 24 h. LC3-GFP–transfected cells were visualized at the indicated time points on the Zeiss Axiovert 200 microscope using the FITC filter.

Generation of Rho zero GBM6 cells. GBM6 cells were cultured in 50 μmol/L of uridine, 1 mmol/L of sodium pyruvate, and the growth medium supplemented with 10 $\mu g/dm^3$ of ethidium bromide. Cells were cultured in this medium for 3 wk before any further experimentation.

Assessment of reactive oxygen species generation. GBM cells were plated in 96-well plates using phenol red–free medium. Cells were preincubated with the peroxide-sensitive fluorescent dye 2′,7′-dichloro-dihydrofluorescein diacetate, or the superoxide-sensitive dye dihydroethidium (5 μmol/L for 30 min; both from Molecular Probes). Intracellular fluorescence measurements for reactive oxygen species (ROS) determination were obtained 0 to 24 h after virus infection with a Vector 3 plate reader. Data are presented corrected for basal fluorescence of vehicle-treated empty well dye blank at each time point (32).

Assessment of cytosolic Ca^{2+} levels. A high-speed wavelength switching fluorescence image analysis system (a Vector 3 plate reader) was used to determine $[Ca^{2+}]_i$ in the carcinoma cells, seeded in 96-well plates (20,000 cells per well), with fura-2 acetoxy-methylester (fura-2) as an indicator. The ratio of fura-2 emissions, when excited at the 340 and 380 nm wavelengths, was recorded and analysis software provided with the Vector 3 plate reader were used to process and statistically analyze data (33).

Published OnlineFirst January 26, 2010; DOI: 10.1158/0008-5472.CAN-09-4043

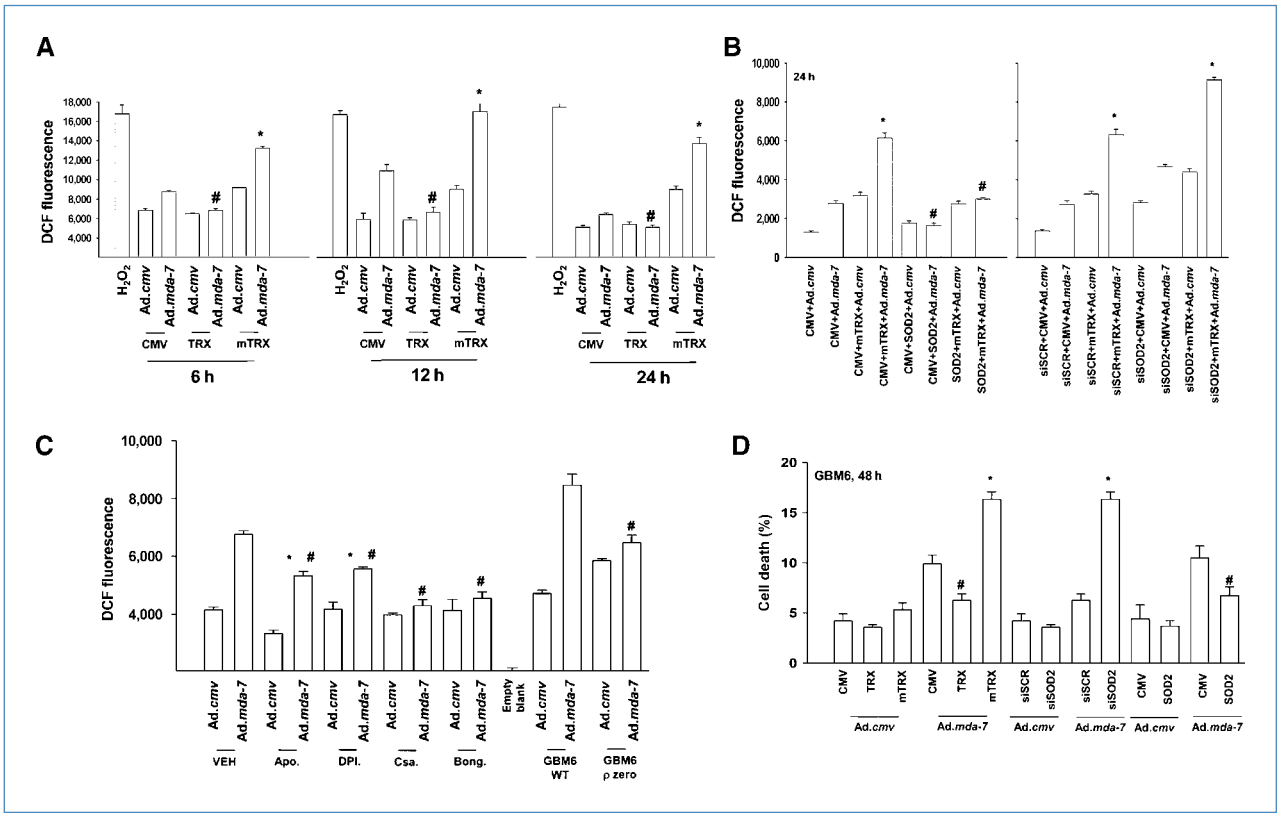

Figure 1. MDA-7/IL-24 promotes mitochondrial ROS generation. A, GBM6 cells transfected with empty vector plasmid (CMV) or plasmids to express wild-type or mutant TRX. Twelve hours later, cells were infected with Ad.*cmv* or with Ad.*mda-7*. The levels of ROS were measured 6, 12, and 24 h after virus infection ($n = 12$, three experiments ± SEM). *, $P < 0.05$ greater than parallel CMV transfection; #, $P < 0.05$ less than parallel CMV transfection. B, GBM6 cells transfected with expression plasmids: CMV, mutant TRX, or SOD2; or with siRNA molecules: scrambled (siSCR) or siSOD2. Twelve hours later, cells were infected with Ad.*cmv* or Ad.*mda-7*. The levels of ROS were measured 24 h after virus infection ($n = 8$, three experiments ± SEM). *, $P < 0.05$ greater than parallel CMV transfection; #, $P < 0.05$ less than parallel CMV transfection. C, GBM6 cells infected with Ad.*cmv* or Ad.*mda-7*. Twelve hours after infection, cells were treated as indicated with vehicle (DMSO), apocynin (Apo., 30 μmol/L), diphenyleneiodonium (DPI., 10 μmol/L), cyclosporine A (Csa, 100 nmol/L), and bongkrekic (Bong., 10 μmol/L), and 30 min after drug treatment, the levels of ROS were measured ($n = 6$, three experiments ± SEM). *, $P < 0.05$ greater than parallel vehicle control; #, $P < 0.05$ less than parallel Ad.*mda-7* infection. D, GBM6 cells transfected with expression plasmids: CMV, mutant TRX, or SOD2; or with siRNA molecules: scrambled (siSCR) or siSOD2. Twelve hours later, cells were infected with Ad.*cmv* or Ad.*mda-7*. Forty-eight hours after infection, viability was determined (± SEM, $n = 3$). *, $P < 0.05$ greater than corresponding Ad.*cmv* value; #, $P < 0.05$ less than parallel CMV transfection.

Mass spectrometric determination of ceramide/dihydroceramide levels. GBM cells were infected/transfected with plasmids and were scraped into PBS 12 h after infection. Lipids were isolated from the cells and ceramide isoforms analyzed by tandem mass spectrometry (34, 35).

Data analysis. Comparison of the *in vitro* effects of various treatments was performed using one-way ANOVA and a two-tailed Student's *t* test. Differences at $P < 0.05$ were considered statistically significant. Experiments shown are the means of multiple individual points from multiple experiments (±SEM).

Results

Expression of MDA-7/IL-24 increased thioredoxin (TRX) and manganese superoxide dismutase 2 (SOD2) protein levels, but not of SOD1 (Supplementary Fig. S1). Expression of MDA-7/IL-24 increased the production of ROS (peroxide) as judged using 2′,7′-dichloro-dihydrofluorescein diacetate that was suppressed by the overexpression of TRX or SOD2, and was enhanced by the expression of mutant inactive TRX or by knockdown of SOD2 levels (Fig. 1A and B; Supplementary Fig. S2). Similar data were obtained examining ROS (superoxide) as judged using dihydroethidium (data not shown). MDA-7/IL-24–induced ROS levels peaked 12 hours after infection, slightly delayed by several hours from the earliest detectable induction of MDA-7/IL-24 protein (Supplementary Fig. S1).

Inhibition of mitochondrial function using small molecule inhibitors or using mitochondria-deficient Rho zero cells, reduced MDA-7/IL-24–induced levels of ROS, whereas small molecule–mediated inhibition of cytosolic NADPH oxidases had little effect on ROS (Fig. 1C). In agreement with the concept that increased ROS levels are toxic, expression of TRX or SOD2 suppressed Ad.*mda-7*–induced killing and expression of mutant TRX or knockdown of SOD2 enhanced

Published OnlineFirst January 26, 2010; DOI: 10.1158/0008-5472.CAN-09-4043

Ad.*mda-7*–induced lethality (Fig. 1D). In colony formation expression of thioredoxin reductase or TRX enhanced survival against Ad.*mda-7*, whereas expression of mutant TRX reduced colony formation (Supplementary Fig. S3).

We examined the effect of manipulating ROS levels on Ad.*mda-7*–induced ER stress, autophagy, and signal transduction. TRX suppressed Ad.*mda-7*–induced Beclin1 and LC3-II expression, the activation of protein kinase R–like endoplasmic reticulum kinase (PERK), eIF2α and JNK1-3, and ERK1/2 and AKT inactivation (Fig. 2A). Expression of mutant TRX enhanced MDA-7/IL-24–induced Beclin1, ATG5, and LC3-II expression; enhanced PERK, eIF2α, p38 MAPK, and JNK1-3 phosphorylation, and abolished ERK1/2 and AKT phosphorylation. TRX binds to the MAP3K upstream of JNK1-3, apoptosis signaling kinase 1, and ROS-induced inactivation of TRX promotes apoptosis signaling kinase 1 activation (32).Expression of dominant negative apoptosis signaling kinase 1 blocked MDA-7/IL-24–induced activation of JNK1-3 (Supplementary Fig. S4). Twelve hours after infection of Ad.*mda-7* in control cells, ROS levels were increased; however, we did not observe increased LC3-GFP vesicularization at this time, indicative of autophagy (Fig. 2B). Ad.*mda-7* infection produced measurable increases in autophagy 24 to 48 hours after infection. Expression of TRX suppressed MDA-7/IL-24–induced LC3-GFP vesicularization, whereas expression of mutant TRX increased vesicularization. Knockdown of Beclin1 or ATG5 expression blocked autophagy and nearly abolished Ad.

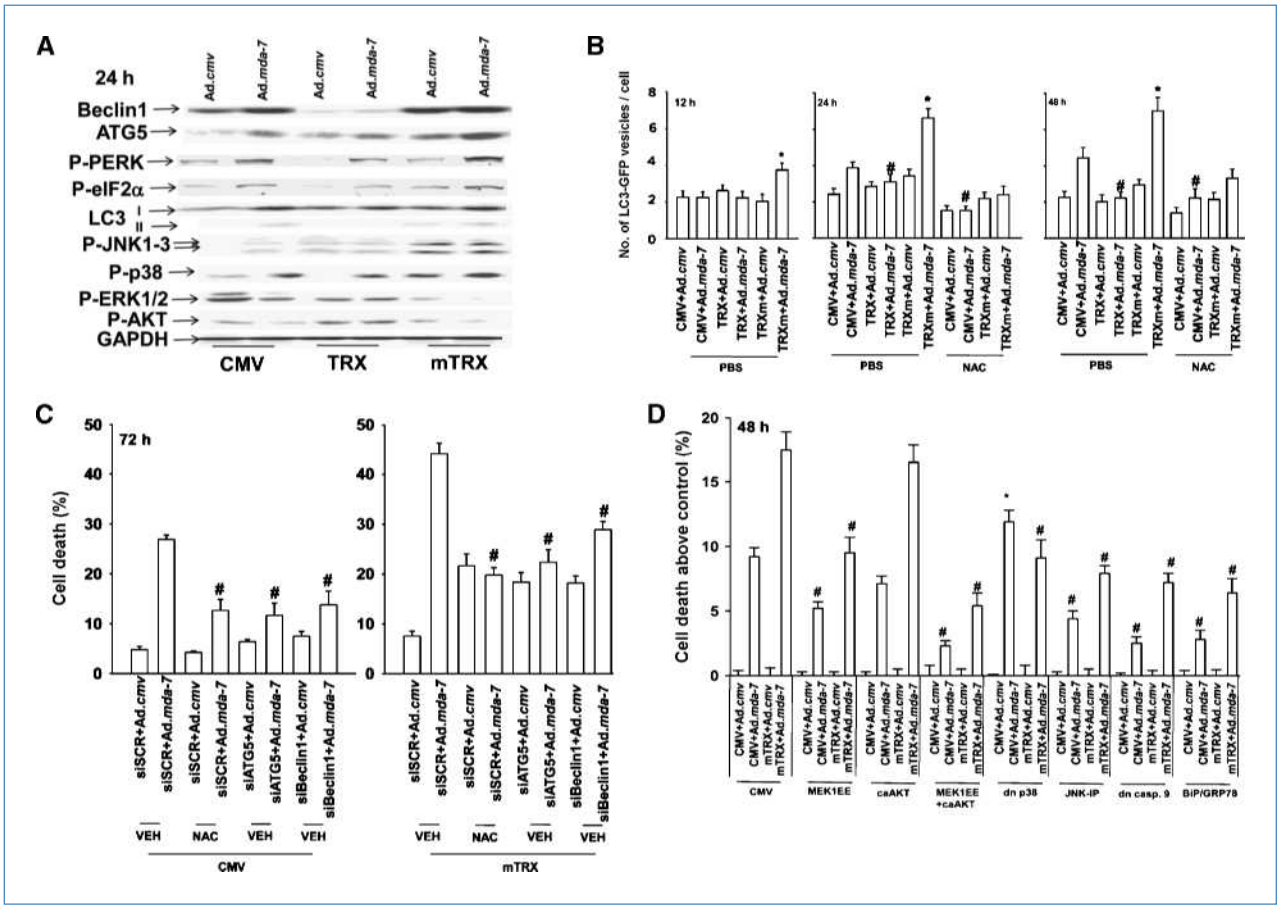

Figure 2. MDA-7/IL-24 promotes autophagy via ROS signaling. A, GBM6 cells transfected with vector plasmid (CMV) or to express wild-type or mutant TRX. Twelve hours later, cells were infected with Ad.*cmv* or Ad.*mda-7*. Twenty-four hours after infection, cells were isolated and subjected to SDS-PAGE and immunoblotting to determine the expression and/or the phosphorylation of the indicated proteins ($n = 3$). B, GBM6 cells transfected with vector plasmid (CMV) or plasmids to express wild-type or mutant TRX; all cells were transfected with a plasmid to express LC3-GFP. Following transfection, cells were treated with vehicle (PBS) or with *N*-acetyl cysteine (10 mmol/L). Twelve to 48 h after infection, slides were examined for punctate GFP vesicles (±SEM, $n = 3$). *, $P < 0.05$ greater than parallel CMV transfection; #, $P < 0.05$ less than parallel CMV transfection. C, GBM6 cells transfected with CMV plasmid or a plasmid to express mutant TRX and in parallel transfected with siRNA molecules: scrambled (siSCR) or to knock down ATG5 or Beclin1. Twelve hours later, cells were infected with Ad.*cmv* or Ad.*mda-7*. Forty-eight hours after infection, cells were isolated and viability determined (±SEM, $n = 3$). #, $P < 0.05$ less than parallel siSCR transfection/vehicle treatment. D, GBM6 cells transfected with CMV plasmid or a plasmid to express BiP/GRP78. Twelve hours later, cells were infected with Ad.*cmv* or Ad.*mda-7*, and in parallel adenoviruses to activate or inhibit MEK1 or AKT or p38 MAPK. Where indicated, cells were treated with the JNK inhibitory peptide (10 μmol/L). Forty-eight hours after infection, cells were isolated and viability determined (±SEM, $n = 3$). *, $P < 0.05$ greater than parallel CMV transfection/infection; #, $P < 0.05$ less than parallel CMV transfection/infection.

Published OnlineFirst January 26, 2010; DOI: 10.1158/0008-5472.CAN-09-4043

mda-7 lethalityand significantly suppressed the enhancement of Ad.*mda-7* lethality by mutant TRX (Fig. 2C; data not shown).

We determined the roles of altered kinase activities in the response of GBM cells to Ad.*mda-7* and mutant TRX expression. Activation of MEK1 or combined activation of MEK1 and AKT suppressed Ad.*mda-7* lethality as well as the enhanced lethality of MDA-7/IL-24 + mutant TRX (Fig. 2D). Inhibition of JNK1-3 or caspase 9 functions, or overexpression of the PERK and MDA-7/IL-24 binding protein BiP/GRP78 (21) suppressed Ad.*mda-7* ± mutant TRX toxicity. Expression of active MEK1 enhanced Ad.*mda-7*–induced BiP/GRP78 levels (Supplementary Fig. S5). Expression of dominant negative p38 MAPK enhanced Ad.*mda-7* lethality; however, blockade of p38 MAPK signaling suppressed the toxic effect of Ad.*mda-7* and mutant TRX.

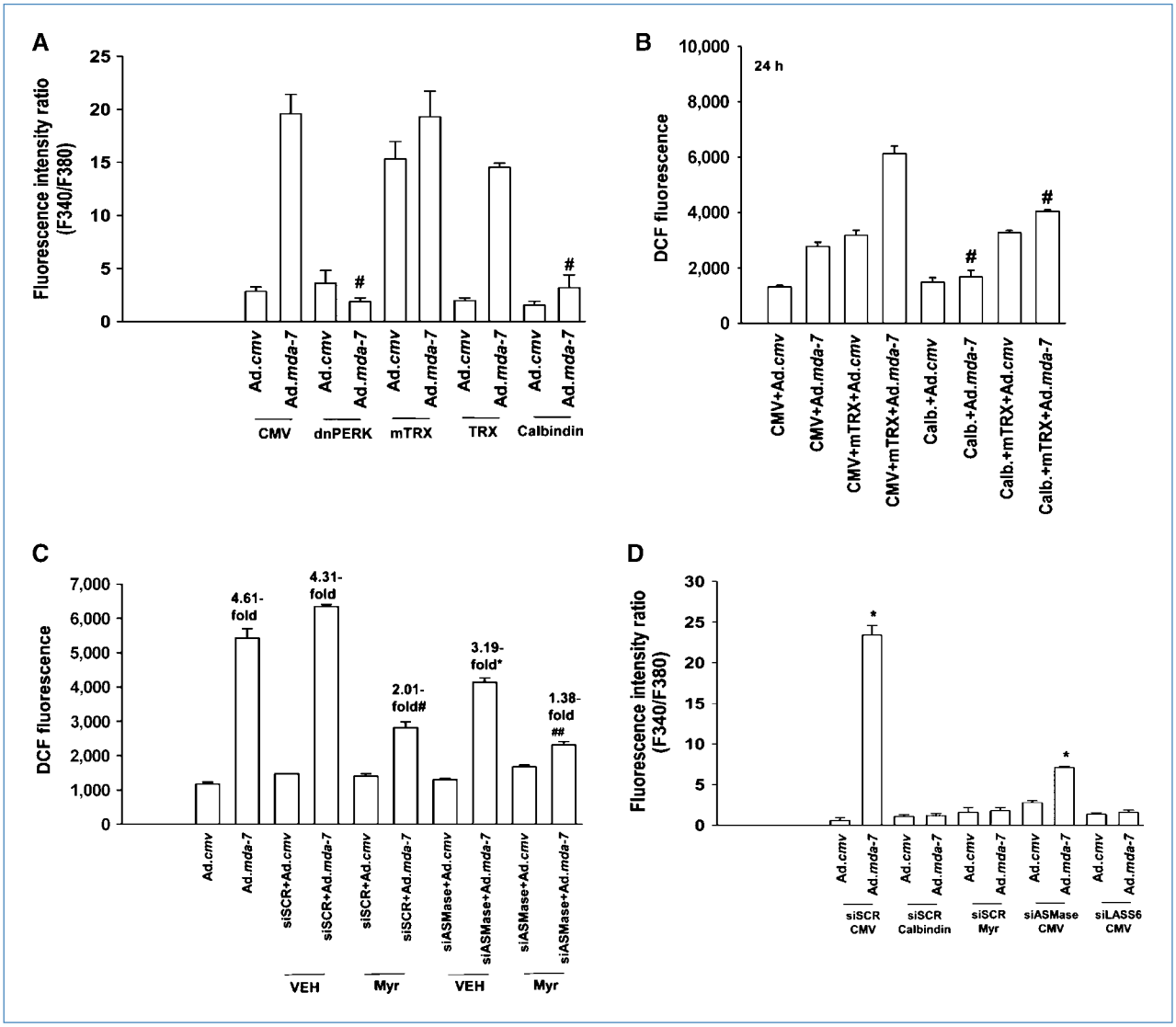

Figure 3. MDA-7/IL-24 increases cytosolic Ca^{2+}, quenching of Ca^{2+} blocks ROS, and inhibition of *de novo* ceramide synthesis blocks enhanced Ca^{2+}. A, GBM6 cells transfected with plasmids: CMV, or to express TRX, mutant TRX, dominant negative PERK or calbindin. Twelve hours later, cells were infected with Ad.*cmv* or Ad.*mda-7*. Twelve hours after infection, levels of cytosolic Ca^{2+} were measured (n = 12, two experiments ± SEM). #, $P < 0.05$ less than parallel CMV transfection. B, GBM6 cells transfected with plasmids: CMV, or to express mutant TRX or calbindin. Twelve hours later, cells infected with Ad.*cmv* or Ad.*mda-7*. Twelve hours after infection, levels of ROS were measured (n = 12, two experiments ± SEM). #, $P < 0.05$ less than parallel CMV transfection. C, GBM6 cells were transfected with CMV or a plasmid to express mutant TRX and in parallel transfected with siRNA molecules: scrambled (siSCR) or to knockdown ASMase. Twelve hours later, cells were infected with Ad.*cmv* or with Ad.*mda-7* and in parallel treated with vehicle (DMSO) or with myriocin (Myr, 1 μmol/L). Twelve hours after infection, levels of ROS were measured (n = 12, two experiments ± SEM). *, $P < 0.05$ greater than parallel Myr treatment; #, $P < 0.05$ less than corresponding vehicle-treated values; ##, $P < 0.05$ less than corresponding value in Myr + siSCR cells. D, GBM6 cells transfected with plasmids: CMV, or to express siLASS6 or calbindin. Twelve hours later, cells infected with Ad.*cmv* or Ad.*mda-7*, and in parallel treated with vehicle (DMSO) or with myriocin (Myr, 1 μmol/L). Twelve hours after infection, levels of cytosolic Ca^{2+} were measured (n = 12, two experiments ± SEM). *, $P < 0.05$ greater than parallel Ad.*cmv* infection.

Published OnlineFirst January 26, 2010; DOI: 10.1158/0008-5472.CAN-09-4043

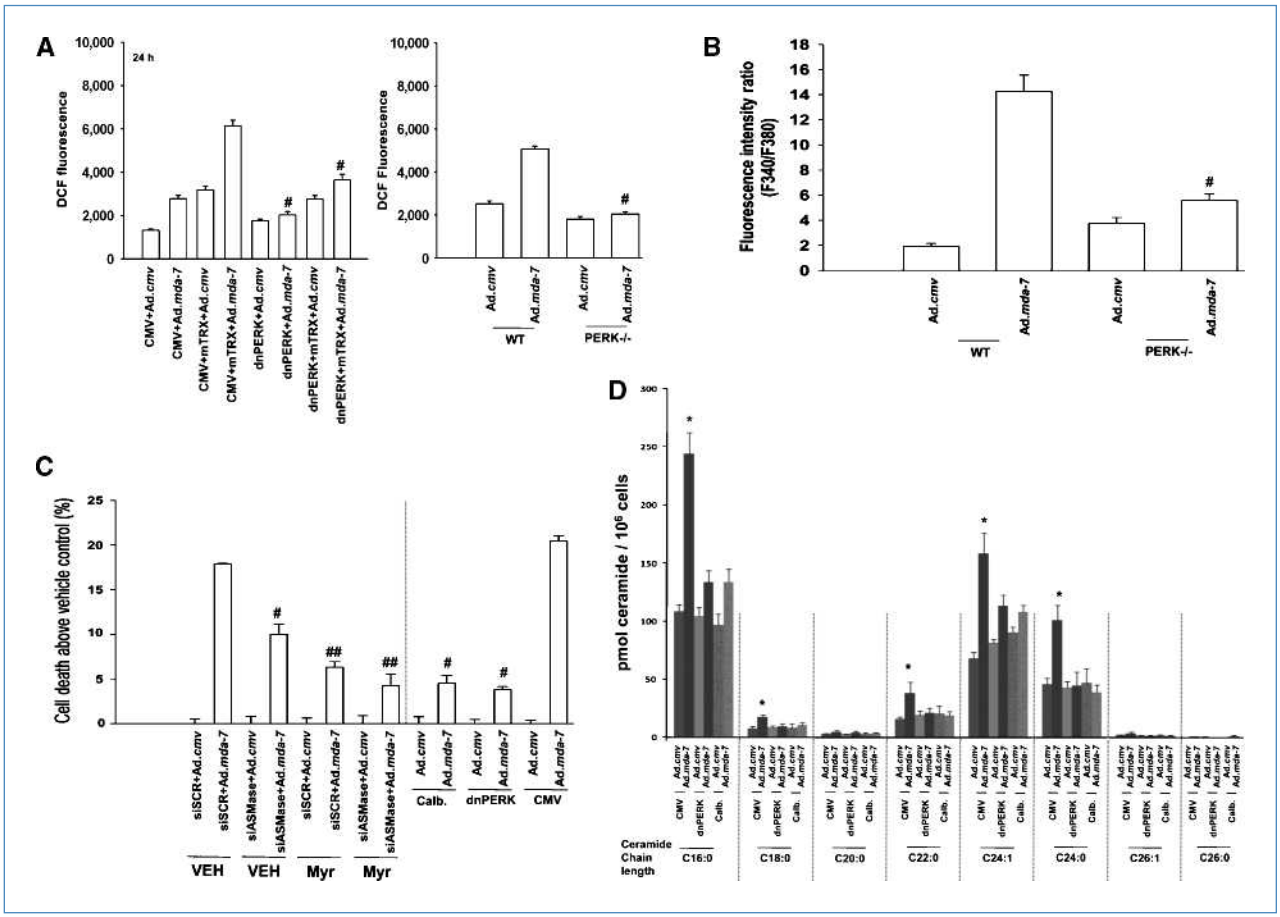

Figure 4. Loss of PERK function blocks MDA-7/IL-24–induced increases in Ca^{2+} and ROS, and cell killing. A, left, GBM6 cells transfected with plasmids: CMV; to express mutant TRX or dominant negative PERK. Twelve hours later, cells were infected with Ad.*cmv* or Ad.*mda-7*. Twelve hours after infection, levels of ROS were measured ($n = 12$, two experiments ± SEM). Right, SV40-transformed MEFs were infected with Ad.*cmv* or Ad.*mda-7*. Twelve hours after infection, levels of ROS were measured ($n = 12$, two experiments ± SEM). #, $P < 0.05$ less than corresponding CMV transfected value. B, SV40-transformed MEFs were infected with Ad.*cmv* or Ad.*mda-7*. Twelve hours after infection, levels of cytosolic Ca^{2+} were measured ($n = 12$, two experiments ± SEM). #, $P < 0.05$ less than corresponding wild-type MEF value. C, left, GBM6 cells were transfected with siRNA molecules: scrambled (siSCR) or to knock down ASMase. Twelve hours later, cells were infected with Ad.*cmv* or Ad.*mda-7* and in parallel treated with vehicle (DMSO) or with myriocin (Myr, 1 μmol/L). Forty-eight hours after infection, cells were isolated and viability determined (±SEM, $n = 3$). ##, $P < 0.05$ less than corresponding vehicle value; #, $P < 0.05$ less than corresponding siSCR value. Right, GBM6 cells were transfected with plasmids: CMV; to express calbindin D28 or dominant negative PERK. Twelve hours later, cells were infected with Ad.*cmv* or Ad.*mda-7*. Forty-eight hours after infection, cells were isolated and viability determined (±SEM, $n = 3$). #, $P < 0.05$ less than corresponding CMV transfected value. D, GBM6 cells were transfected with plasmids: CMV, or to express calbindin D28 or dominant negative PERK. Twelve hours later, cells were infected with Ad.*cmv* or Ad.*mda-7*. Twelve hours after infection, cells were scraped into PBS, the cells lysed and lipids extracted prior to analyses by tandem mass spectrometry ($n = 4$; three experiments ± SEM). *, $P < 0.05$ greater than Ad.*cmv* control.

We determined whether MDA-7/IL-24 caused any changes in the cytosolic levels of Ca^{2+}. Ad.*mda-7* infection increased cytosolic Ca^{2+} levels within 12 hours (Fig. 3A). The increase in Ca^{2+} was blocked by dominant negative PERK or calbindin D28 expression, but was not altered by TRX toxicity expression. Calbindin D28 expression blocked Ad.*mda-7*–induced ROS and blunted the ability of mutant TRX to further increase ROS levels (Fig. 3B). Infection of GBM cells with Ad.*mda-7* promoted eEF2 phosphorylation that was blocked by expression of calbindin (Supplementary Fig. S6; ref. 36).

Prior studies examining the effects of MDA-7/IL-24 in carcinoma cells has shown that ceramide generation plays a key role in cytokine lethality (32, 35). Inhibition of the *de novo* ceramide synthesis pathway, and to a lesser extent, the acidic sphingomyelinase (ASMase) pathway, significantly reduced Ad.*mda-7*–induced ROS levels (Fig. 3C). Similar data were obtained when ceramide synthase 6 (LASS6) expression was knocked down (data not shown). Inhibition of the *de novo* ceramide synthesis pathway using myriocin or knockdown of LASS6 blocked Ad.*mda-7*–induced changes in cytosolic Ca^{2+}, whereas ASMase inhibition only partially blunted Ca^{2+} (Fig. 3D).

The mechanism by which Ad.*mda-7* increased dihydroceramide levels was explored using a vector to express a FLAG-tagged LASS6. Infection of FLAG-LASS6–transfected cells with Ad.*cmv* did not alter FLAG-LASS6 levels compared with uninfected cells (Supplementary Fig. S7). More noticeably, infection of cells with Ad.*mda-7* caused a large increase in

Published OnlineFirst January 26, 2010; DOI: 10.1158/0008-5472.CAN-09-4043

FLAG-LASS6 protein levels. As FLAG-LASS6 was being expressed from a plasmid using a constitutively active cytomegalovirus promoter, our data suggest that expression of MDA-7/IL-24 stabilized LASS6 mRNA/protein levels. Expression of dominant negative PERK reduced Ad.*mda-7*–induced LASS6 levels by 63 ± 3% ($P < 0.05$).

Expression of dominant negative PERK or knockout of PERK abolished Ad.*mda-7*–induced ROS levels, and knockout of PERK blocked Ad.*mda-7*–induced cytosolic Ca^{2+} changes (Fig. 4A and B). Inhibition of *de novo* ceramide synthesis; inhibition of changes in cytosolic Ca^{2+}; or expression of dominant negative PERK suppressed Ad.*mda-7* lethality (Fig. 4C). Expression of MDA-7/IL-24 rapidly increased ceramide and dihydroceramide levels within 12 hours, which was suppressed by >80% by dominant negative PERK or by knockdown of LASS6 (Fig. 4D; Supplementary Fig. S8; data not shown). Calbindin D28 expression blocked MDA-7/IL-24–induced ceramide but did not alter MDA-7/IL-24–induced dihydroceramide levels.

Radiotherapy is a primary modality in GBM treatment. Ad.*mda-7* enhanced the toxicity of ionizing radiation in a dose-dependent fashion (Fig. 5A). Radiation enhanced the vesicularization of LC3-GFP and combined with Ad.*mda-7* infection caused an at least additive increase in LC3-GFP vesicle numbers (Fig. 5B). The ability of radiation to increase vesicle formation was blocked by the expression of calbindin D28, TRX, or dominant negative PERK; or by knockdown of LASS6 (data not shown). Knockdown of ATG5 or Beclin1 suppressed autophagy and reduced, although it did not abolish, the toxic interaction between MDA-7/IL-24 and radiation (Fig. 5C). In colony assays, knockdown of ATG5 or Beclin1 almost abolished the toxicity of either Ad.*mda-7* or radiation; however, combined MDA-7/IL-24 and radiation exposure, even in the absence of autophagy, was still capable of causing a significant survival reduction (Fig. 5D). Knockdown of Beclin1 suppressed MDA-7/IL-24–induced cytosol release of cytochrome *c*, and partially suppressed the release caused by MDA-7/IL-24 + radiation exposure (Supplementary Fig. S9).

Inhibition of TRX has been postulated to improve the therapeutic effects of chemotherapeutic drugs, and TRX inhibitors are undergoing phase I evaluation (37). Infection of GBM6 cells with Ad.*mda-7* suppressed tumor formation, as did transfection with mutant TRX (Supplementary Fig. S10). GBM cells expressing both MDA-7/IL-24 and mutant TRX did not form progressive tumors for up to 28 days postimplantation. Animals infected with Ad.*cmv* + vector had a mean survival of 38 ± 7 days; animals infected with Ad.*cmv* + mTRX had a mean survival of 47 ± 4 days; animals infected with Ad.*mda-7* + vector had a mean survival of 79 ± 9 days; animals infected with Ad.*mda-7* + mTRX were *all* viable 110 days postimplantation ($P < 0.05$ different from Ad.*mda-7* + vector).

Discussion

Previous studies have noted that MDA-7/IL-24 reduces proliferation and causes tumor cell–specific killing and radiosensitization (20). Although PERK-dependent autophagy and JNK-signaling plays a key role in killing by *mda-7*/IL-24 of GBM cells, the precise pathways proximally downstream of PERK activation provoked by Ad.*mda-7* and causally related to its cancer-specific cell killing effects require further clarification. The studies in this article were designed to define precisely how GBM cells respond to MDA-7/IL-24.

Infection of GBM cells with Ad.*mda-7* that caused ~30% apoptosis in 72 hours correlated with the induction of ceramide, dihydroceramide, cytosolic Ca^{2+}, and ROS 12 hours after infection. The increased levels of ceramide, dihydroceramide, cytosolic Ca^{2+}, and ROS were blocked by the expression of dominant negative PERK. Inhibition of ceramide generation blocked increased cytosolic Ca^{2+} and ROS levels and quenching of cytosolic Ca^{2+} blocked the induction of ROS. Quenching of Ca^{2+} also inhibited MDA-7/IL-24–induced ceramide production. Quenching of Ca^{2+} did not block MDA-7/IL-24–induced dihydroceramide levels and MDA-7/IL-24 increased the expression of ceramide synthase 6. Inhibition of mitochondrial respiratory function blocked increased ROS, and quenching of ROS blocked MDA-7/IL-24–induced autophagy. Genetic suppression of autophagy blocked Ad.*mda-7* toxicity. Our data favors a model for MDA-7/IL-24 actions in GBM cells in which MDA-7/IL-24, by disrupting the interaction between PERK and its chaperone BiP/GRP78, causes PERK to become activated which promotes dihydroceramide generation followed by a codependent induction of Ca^{2+} and ceramide, leading to greater levels of cytosolic Ca^{2+} that affects mitochondria to generate ROS; elevated ROS levels stimulate toxic autophagy leading to tumor cell death (Supplementary Fig. S11).

PERK signaling could promote tumor cell death or survival based on the stimulus (e.g., refs. 24, 25, 38, 39). There are three primary unfolded protein response sensors: PERK, activating transcription factor 6, and inositol-requiring enzyme 1. As unfolded proteins accumulate, BiP/GRP78, the HSP70 ER-resident chaperone, dissociates from PERK, activating transcription factor 6, or IRE1. BiP/GRP78 dissociation from PERK allows this protein to dimerize, autophosphorylate, and then phosphorylate eIF2α, the protein required for bringing the initiator methionyl-tRNA to the 40S ribosome (25). Phosphorylated eIF2α leads to the repression of global translation, helping cells to recover from the accumulation of unfolded proteins. Reduced translation can also lower the expression of short-lived prosurvival proteins such as MCL-1. MDA-7/IL-24 binds to BiP/GRP78, and in GBM cells, we hypothesized that this binding would play a central role in regulating PERK activity and regulating MDA-7/IL24–induced killing (21, 25, 32). A constitutively active form of MEK1 maintained ERK1/2 phosphorylation in cells expressing MDA-7/IL-24, increased BiP/GRP78 expression, blocked PERK activation, and reduced MDA-7/IL-24 lethality. Overexpression of BiP/GRP78 blocked MDA-7/IL-24–induced PERK activation and tumor cell death. Expression of dominant negative PERK blocked MDA-7/IL-24–induced activation of eIF2α and JNK1-3 as well as reduced expression of MCL-1. Thus, in GBM cells MDA-7/IL-24, by binding to BiP/GRP78, results in the disruption of the BiP/GRP78-PERK chaperone interaction resulting in enhanced PERK signaling into

Published OnlineFirst January 26, 2010; DOI: 10.1158/0008-5472.CAN-09-4043

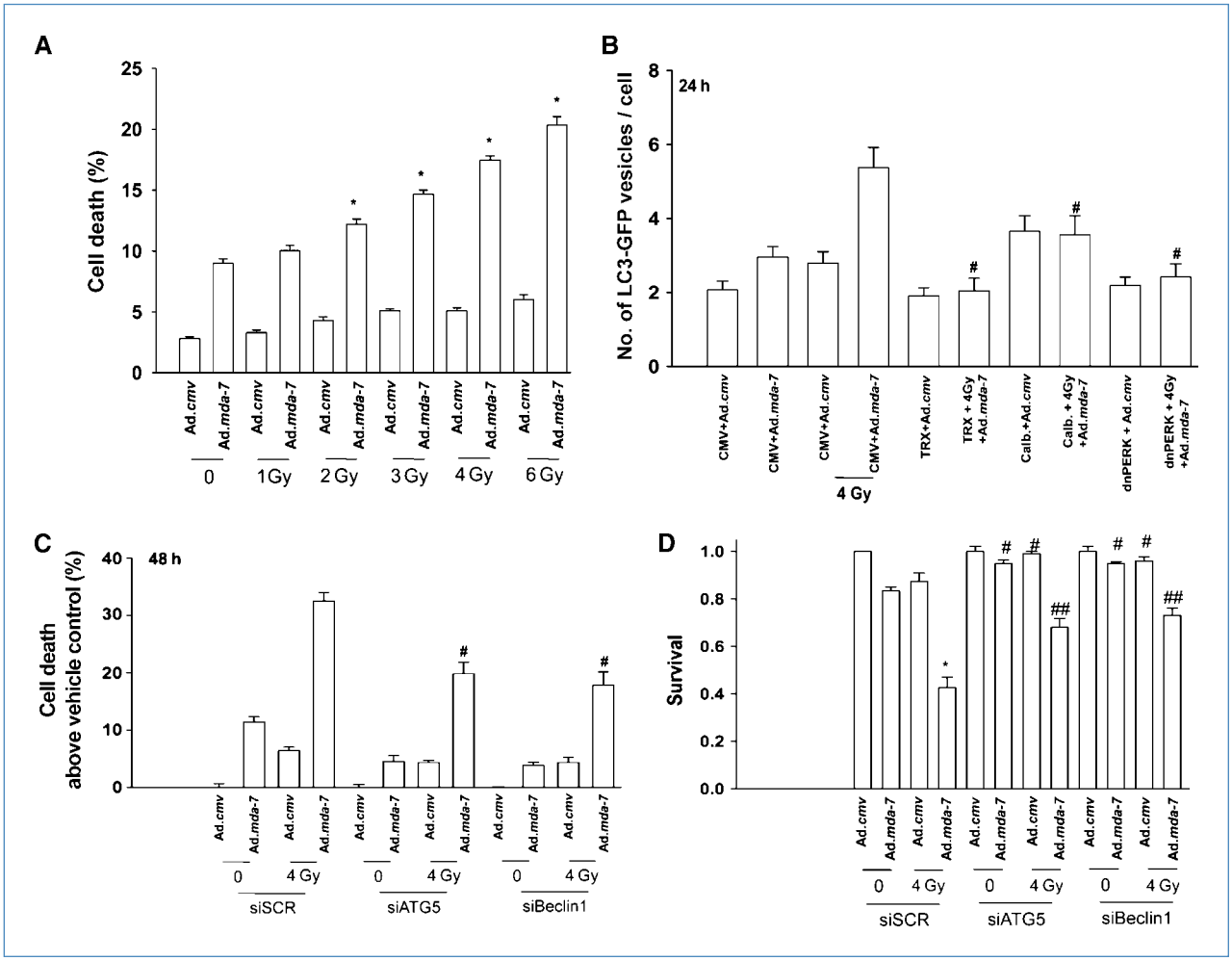

Figure 5. MDA-7/IL-24 radiosensitizes GBM cells through a ceramide/Ca^{2+}/ROS–dependent mechanism that is partially dependent on altered levels of autophagy. A, GBM6 cells infected with Ad.*cmv* or with Ad.*mda-7* and 12 h later irradiated (0–6 Gy). Cells were isolated 48 h after infection and viability determined (±SEM, $n = 3$). *, $P < 0.05$ greater differential between Ad.*cmv* and Ad.*mda-7* values in unirradiated cells. B, GBM6 cells transfected with plasmids: to express LC3-GFP and to express nothing, TRX, calbindin D28, or dominant negative PERK. Twelve hours later, cells were infected with Ad.*cmv* or Ad.*mda-7*. Twenty-four hours after infection, slides were examined for punctate GFP vesicles (±SEM, $n = 3$). #, $P < 0.05$ less than corresponding value in CMV-transfected irradiated cells. C, GBM6 cells transfected: scrambled (siSCR) or to knock down ATG5 or Beclin1. Twelve hours later, cells were infected with Ad.*cmv* or Ad.*mda-7*. Forty-eight hours after infection, cells viability determined (±SEM, $n = 3$). #, $P < 0.05$ less than corresponding value in siSCR transfected cells. D, GBM6 cells were transfected with siRNA molecules: scrambled (siSCR) or to knock down ATG5 or Beclin1. Twelve hours later, cells were infected with Ad.*cmv* or Ad.*mda-7* and 12 h later were irradiated (4 Gy) and the plates incubated for a further ~20 d to permit colonies of >50 cells to form (±SEM, $n = 3$). *, $P < 0.05$ greater reduction in colony formation than Ad.*mda-7* or irradiation; #, $P < 0.05$ less than corresponding value in siSCR cells; ##, $P < 0.05$ greater reduction in colony formation than Ad.*mda-7* or irradiation alone and less than corresponding value in siSCR cells.

the eIF2α and JNK pathways that act to promote mitochondrial dysfunction.

The production of ROS was also essential in the regulation of ERK1/2, AKT, JNK1-3, and p38 MAPK by MDA-7/IL-24, with overexpression of TRX blocking inhibition of ERK1/2 and AKT, and blunting the activation of JNK1/2 and p38 MAPK, and conversely, the expression of mutant TRX facilitating the inactivation of ERK1/2 and AKT and greater activation of JNK1-3 and p38 MAPK. Multiple studies using a variety of cytokine and toxic stimuli document that prolonged JNK1-3 and/or p38 MAPK activation in a wide variety of cell types could trigger apoptosis (40). TRX can reduce many oxidized proteins and it supports a large system of redox detoxification reactions. Sequential univalent transfer occurs with many redox proteins that generate superoxide species so that hydrogen peroxide is a common product of these reactions. Dismutation of the superoxide anion to hydrogen peroxide and oxygen occurs at a rapid rate and the reaction of radicals with radical scavengers such as TRX results in a highly efficient conversion of radicals to nonradical oxidants such as hydrogen peroxide (41).

In addition to modulating the activities of signal transduction pathways, inhibiting ROS detoxification *in vitro* enhanced MDA-7/IL-24–induced ROS levels that promoted greater

Published OnlineFirst January 26, 2010; DOI: 10.1158/0008-5472.CAN-09-4043

autophagy levels. The mechanisms by which elevated ROS levels regulate autophagy are not fully understood. There are multiple possibilities for radical species to alter ER stress levels. Reactive nitrogen species could inhibit protein disulfide isomerase activity, leading to increased protein unfolding in the ER and activation of PERK and JNK1/2 with resultant cell killing (42). The PI3P lipid phosphatase "Jumpy" negatively regulates autophagy and it is known that lipid and tyrosine phosphatase activities are inactivated by elevated ROS levels (43, 44).

MDA-7/IL-24 and ionizing radiation interact in a greater than additive fashion to kill GBM cells *in vitro* and *in vivo*. As has been noted by others, we found that exposure of primary human GBM cells to radiation increased LC3-GFP vesicle levels within 24 hours (45). Some studies have argued that radiation-induced autophagy is a protective effect following exposure, whereas others have argued that autophagy plays a role in radiosensitization (46, 47). Our data argued that ATG5 or Beclin1 knockdown suppressed radiation toxicity in GBM cells. Radiation and MDA-7/IL-24 interacted to cause a greater than additive induction of autophagic vesicles in GBM cells and suppression of ceramide, Ca^{2+}, or ROS signaling abolished the MDA-7/IL-24 + radiation-induced increase in autophagy. However, whereas inhibition of autophagy suppressed the toxic effects of MDA-7/IL-24 or radiation in colony formation assays to a level approaching those observed in control-treated cells, the combination of MDA-7/IL-24 + radiation still exhibited a significant, albeit reduced, amount of killing. Prior analyses have shown that MDA-7/IL-24 + radiation toxicity is completely blocked by pan-caspase inhibitors and inhibitors of the intrinsic apoptosis pathway. Measurable radiation-induced increases in ROS levels in tumor cells are known to be dependent on functional mitochondria acting as amplifiers of ROS that act to promote MDA-7/IL-24–induced activation of JNK1-3, and subsequently, BAX and BAK (24, 25). Our findings argue that radiation enhances MDA-7/IL-24 toxicity via promoting increased autophagy, and in a direct manner, via elevated JNK signaling with increased cytochrome *c* release from the mitochondrion.

Expression of dominant negative PERK suppressed ceramide generation in GBM cells, which implies either that PERK directly or indirectly through its kinase phosphorylates ASMase and/or ceramide synthase 6 to regulate their activity or that activation of PERK via eIF2α modulates the expression of proteins which result in elevated ER-localized ceramide activity. In this regard, both acid and neutral ceramidase enzymes are known to be regulated by transcription and have ~6 hours half-life (48). However, preliminary assays noted that acid ceramidase levels did not decrease in response to MDA-7/IL-24 expression. In contrast, we found that MDA-7/IL-24 expression increased the protein levels of FLAG-tagged LASS6. As FLAG-LASS6 is expressed using a constitutively active promoter, these findings argue that MDA-7/IL-24 promotes the stabilization of LASS6 mRNA and/or protein. The precise ER and mitochondrial targets of MDA-7/IL-24–induced ceramide generation in GBM cells will need to be examined in detail in future studies.

Disclosure of Potential Conflicts of Interest

No potential conflicts of interest were disclosed.

Grant Support

P01-CA104177, R01-CA108325, R01-DK52825; R01-CA63753, R01-CA77141, R01-CA097318; R01-CA098712; P01-NS031492. P. Dent is a Universal Professor in Signal Transduction and P.B. Fisher holds the Thelma Newmeyer Corman Chair in Cancer Research and is a Samuel Waxman Cancer Research Foundation Investigator.

The costs of publication of this article were defrayed in part by the payment of page charges. This article must therefore be hereby marked *advertisement* in accordance with 18 U.S.C. Section 1734 solely to indicate this fact.

Received 11/4/09; revised 12/1/09; accepted 12/2/09; published OnlineFirst 1/26/10.

References

1. Robins HI, Chang S, Butowski N, Mehta M. Therapeutic advances for glioblastoma multiforme: current status and future prospects. Curr Oncol Rep 2007;9:66–70.
2. Jiang H, Lin JJ, Su ZZ, Goldstein NI, Fisher PB. Subtraction hybridization identifies a novel melanoma differentiation associated gene, *mda-7*, modulated during human melanoma differentiation, growth and progression. Oncogene 1995;11:2477–86.
3. Ekmekcioglu S, Ellerhorst J, Mhashilkar AM, et al. Down-regulated melanoma differentiation associated gene (*mda-7*) expression in human melanomas. Int J Cancer 2001;94:54–9.
4. Ellerhorst JA, Prieto VG, Ekmekcioglu S. Loss of MDA-7 expression with progression of melanoma. J Clin Oncol 2002;20:1069–74.
5. Huang EY, Madireddi MT, Gopalkrishnan RV, et al. Genomic structure, chromosomal localization and expression profile of a novel melanoma differentiation associated (*mda-7*) gene with cancer specific growth suppressing and apoptosis inducing properties. Oncogene 2001;20:7051–63.
6. Parrish-Novak J, Xu W, Brender T, et al. Interleukins 19, 20, and 24 signal through two distinct receptor complexes. Differences in receptor-ligand interactions mediate unique biological functions. J Biol Chem 2002;277:47517–23.
7. Caudell EG, Mumm JB, Poindexter N, et al. The protein product of the tumor suppressor gene, melanoma differentiation-associated gene 7, exhibits immunostimulatory activity and is designated IL-24. J Immunol 2002;168:6041–6.
8. Pestka S, Krause CD, Sarkar D, Walter MR, Shi Y, Fisher PB. Interleukin-10 and related cytokines and receptors. Annu Rev Immunol 2004;22:929–79.
9. Gupta P, Su ZZ, Lebedeva IV, et al. *mda-7*/IL-24: multifunctional cancer-specific apoptosis-inducing cytokine. Pharmacol Ther 2006;111:596–28.
10. Lebedeva IV, Sauane M, Gopalkrishnan RV, et al. *mda-7*/IL-24: exploiting cancer's Achilles' heel. Mol Ther 2005;11:4–18.
11. Fisher PB, Gopalkrishnan RV, Chada S, et al. *mda-7*/IL-24, a novel cancer selective apoptosis inducing cytokine gene: from the laboratory into the clinic. Cancer Biol Ther 2003;2:S23–37.
12. Fisher PB. Is *mda-7*/IL-24 a "magic bullet" for cancer? Cancer Res 2005;65:10128–38.
13. Su ZZ, Lebedeva IV, Gopalkrishnan RV, et al. A combinatorial approach for selectively inducing programmed cell death in human pancreatic cancer cells. Proc Natl Acad Sci U S A 2001;98:10332–7.
14. Su ZZ, Madireddi MT, Lin JJ, et al. The cancer growth suppressor

gene *mda-7* selectively induces apoptosis in human breast cancer cells and inhibits tumor growth in nude mice. Proc Natl Acad Sci U S A 1998;95:14400–5.
15. Cunningham CC, Chada S, Merritt JA, et al. Clinical and local biological effects of an intratumoral injection of *mda-7* (IL24; INGN 241) in patients with advanced carcinoma: a phase I study. Mol Ther 2005; 11:149–59.
16. Fisher PB, Sarkar D, Lebedeva IV, et al. Melanoma differentiation associated gene-7/interleukin-24 (mda-7/IL-24): novel gene therapeutic for metastatic melanoma. Toxicol Appl Pharmacol 2007;224:300–7.
17. Lebedeva IV, Su ZZ, Chang Y, Kitada S, Reed JC, Fisher PB. The cancer growth suppressing gene *mda-7* induces apoptosis selectively in human melanoma cells. Oncogene 2002;21:708–18.
18. Su ZZ, Lebedeva IV, Sarkar D, et al. Ionizing radiation enhances therapeutic activity of *mda-7*/IL-24: overcoming radiation- and *mda-7*/IL-24-resistance in prostate cancer cells over-expressing the antiapoptotic proteins bcl-x_L or bcl-2. Oncogene 2006;25:2339–48.
19. Gopalan B, Litvak A, Sharma S, Mhashilkar AM, Chada S, Ramesh R. Activation of the Fas-FasL signaling pathway by MDA-7/IL-24 kills human ovarian cancer cells. Cancer Res 2005;65:3017–24.
20. Emdad L, Lebedeva IV, Su ZZ, et al. Historical perspective and recent insights into our understanding of the molecular and biochemical basis of the antitumor properties of *mda*-7/IL-24. Cancer Biol Ther 2009;8:391–400.
21. Gupta P, Walter MR, Su ZZ, et al. BiP/GRP78 Is an intracellular target for MDA-7/IL-24 induction of cancer-specific apoptosis. Cancer Res 2006;66:8182–91.
22. Yacoub A, Mitchell C, Hong Y, et al. MDA-7 regulates cell growth and radiosensitivity *in vitro* of primary (non-established) human glioma cells. Cancer Biol Ther 2004;3:739–51.
23. Yacoub A, Hamed H, Emdad L, et al. MDA-7/IL-24 plus radiation enhance survival in animals with intracranial primary human GBM tumors. Cancer Biol Ther 2008;7:917–33.
24. Yacoub A, Park MA, Gupta P, et al. Caspase-, cathepsin-, and PERK-dependent regulation of MDA-7/IL-24-induced cell killing in primary human glioma cells. Mol Cancer Ther 2008;7:297–13.
25. Yacoub A, Gupta P, Park MA, et al. Regulation of GST-MDA-7 toxicity in human glioblastoma cells by ERBB1, ERK1/2, PI3K, JNK1-3 pathway signaling. Mol Cancer Ther 2008;7:314–29.
26. Yacoub A, Mitchell C, Brannon J, et al. MDA-7 (interleukin-24) inhibits the proliferation of renal carcinoma cells and interacts with free radicals to promote cell death and loss of reproductive capacity. Mol Cancer Ther 2003;2:623–32.
27. Sarkar D, Su ZZ, Lebedeva IV, et al. *mda-7* (IL-24) Mediates selective apoptosis in human melanoma cells by inducing the coordinated over-expression of the GADD family of genes by means of p38 MAPK. Proc Natl Acad Sci U S A 2002;99:10054–9.
28. Mhashilkar AM, Stewart AL, Sieger K, et al. MDA-7 negatively regulates the β-catenin and PI3K signaling pathways in breast and lung tumor cells. Mol Ther 2003;8:207–19.
29. Chada S, Bocangel D, Ramesh R, et al. *mda-7*/IL24 kills pancreatic cancer cells by inhibition of the Wnt/PI3K signaling pathways: identification of IL-20 receptor-mediated bystander activity against pancreatic cancer. Mol Ther 2005;11:724–33.
30. Sauane M, Gopalkrishnan RV, Choo HT, et al. Mechanistic aspects of *mda-7*/IL-24 cancer cell selectivity analysed via a bacterial fusion protein. Oncogene 2004;23:7679–90.
31. Park MA, Zhang G, Norris J, et al. Regulation of autophagy by ceramide-CD95-PERK signaling. Autophagy 2008;4:929–31.
32. Park MA, Walker T, Martin AP, et al. MDA-7/IL-24-induced cell killing in malignant renal carcinoma cells occurs by a ceramide/CD95/PERK-dependent mechanism. Mol Cancer Ther 2009;8:1280–91.
33. Mitchell C, Park MA, Zhang G, et al. 17-Allylamino-17-demethoxygeldanamycin enhances the lethality of deoxycholic acid in primary rodent hepatocytes and established cell lines. Mol Cancer Ther 2007;6:618–32.
34. Park MA, Zhang G, Martin AP, et al. Vorinostat and sorafenib increase ER stress, autophagy and apoptosis via ceramide-dependent CD95 and PERK activation. Cancer Biol Ther 2008;7:1648–62.
35. Sauane M, Su ZZ, Dash R, et al. Ceramide plays a prominent role in MDA-7/IL-24-induced cancer-specific apoptosis. J Cell Physiol 2009;222:546–55.
36. Liang SH, Zhang W, McGrath BC, Zhang P, Cavener DR. PERK (eIF2α kinase) is required to activate the stress-activated MAPKs and induce the expression of immediate-early genes upon disruption of ER calcium homoeostasis. Biochem J 2006;393:201–9.
37. Powis G, Kirkpatrick DL. Thioredoxin signaling as a target for cancer therapy. Curr Opin Pharmacol 2007;7:392–7.
38. Zhang G, Park MA, Mitchell C, et al. Multiple cyclin kinase inhibitors promote bile acid-induced apoptosis and autophagy in primary hepatocytes via p53-95-dependent signaling. J Biol Chem 2008; 283:24343–58.
39. Park MA, Yacoub A, Rahmani M, et al. OSU-03012 stimulates PKR-like endoplasmic reticulum-dependent increases in 70-kDa heat shock protein expression, attenuating its lethal actions in transformed cells. Mol Pharmacol 2008;73:1168–84.
40. Matsuzawa A, Nishitoh H, Tobiume K, Takeda K, Ichijo H. Physiological roles of ASK1-mediated signal transduction in oxidative stress- and endoplasmic reticulum stress-induced apoptosis: advanced findings from ASK1 knockout mice. Antioxid Redox Signal 2002;4: 415–25.
41. Maulik N, Das DK. Emerging potential of thioredoxin and thioredoxin interacting proteins in various disease conditions. Biochim Biophys Acta 2008;1780:1368–82.
42. Townsend DM, Manevich Y, He L, et al. Nitrosative stress-induced s-glutathionylation of protein disulfide isomerase leads to activation of the unfolded protein response. Cancer Res 2009;69: 7626–34.
43. Vergne I, Roberts E, Elmaoued RA, et al. Control of autophagy initiation by phosphoinositide 3-phosphatase jumpy. EMBO J 2009;28: 2244–58.
44. Fang Y, Han SI, Mitchell C, et al. Bile acids induce mitochondrial ROS, which promote activation of receptor tyrosine kinases and signaling pathways in rat hepatocytes. Hepatology 2004;40:961–71.
45. Yao KC, Komata T, Kondo Y, Kanzawa T, Kondo S, Germano IM. Molecular response of human glioblastoma multiforme cells to ionizing radiation: cell cycle arrest, modulation of the expression of cyclin-dependent kinase inhibitors, and autophagy. J Neurosurg 2003;98:378–84.
46. Gewirtz DA, Hilliker ML, Wilson EN. Promotion of autophagy as a mechanism for radiation sensitization of breast tumor cells. Radiother Oncol 2009;92:323–8.
47. Lomonaco SL, Finniss S, Xiang C, et al. The induction of autophagy by γ-radiation contributes to the radioresistance of glioma stem cells. Int J Cancer 2009;125:717–22.
48. Mao C, Obeid LM. Ceramidases: regulators of cellular responses mediated by ceramide, sphingosine, and sphingosine-1-phosphate. Biochim Biophys Acta 2008;1781:424–34.

Cancer Research
The Journal of Cancer Research (1916–1930) | The American Journal of Cancer (1931–1940)

AACR American Association for Cancer Research

PERK–Dependent Regulation of Ceramide Synthase 6 and Thioredoxin Play a Key Role in *mda*-7/IL-24–Induced Killing of Primary Human Glioblastoma Multiforme Cells

Adly Yacoub, Hossein A. Hamed, Jeremy Allegood, et al.

Cancer Res 2010;70:1120-1129. Published OnlineFirst January 26, 2010.